Grid Friendly Operation of a PV-Storage System with Profit Maximization and Reliability Enhancement

Lysandros Tziovani, Panayiotis Kolios, Lenos Hadjidemetriou and Elias Kyriakides
KIOS Research and Innovation Center of Excellence and Department of Electrical and Computer Engineering
University of Cyprus
Nicosia, Cyprus
Email: {ltziov01, pkolios, hadjidemetriou.lenos, elias}@ucy.ac.cy

***Abstract*—The intermittent character of renewable energy sources (RES) creates market potentials for the emerging energy storage technologies. Energy storage systems can be utilized to support the grid, compensate the intense variation of RES production, and create opportunities for prosumers to maximize their profit under a variable electricity pricing scheme. In this paper, an optimal scheduling method is designed for a hybrid photovoltaic-storage system in a non-residential building. The scheduling scheme defines the utilization of a flywheel based storage device to minimize the cost of the electricity bill and simultaneously reduces the peak power exchange with the grid for a smooth power interaction. Further, the method considers the lifetime extension of the hybrid system grid-tied inverter by limiting the maximum output power of the inverter, without any energy shedding of solar power. The proposed optimization problem is solved for the day ahead using predicted input data. Several case studies are examined and useful results are obtained according to the profit and the grid interaction of the prosumer.**

***Index Terms*—Energy management, grid interaction, inverter lifetime, mixed-integer linear programming, optimization.**

NOMENCLATURE

Indices/Sets

T	Set of optimization time intervals.
N	Set of linear segments of the piecewise linearization for the inverter efficiency curve.
t	Index for time intervals.
k	Index for linear segments.

Parameters

$c_{buy}(t)$	Cost of power purchased by the grid in €/kWh.
$c_{sell}(t)$	Cost of power sold to the grid in €/kWh.
$L(t)$	Load demand in kW.
$P_{PV}(t)$	Power generated by the PV system in kW.
$x_p(k)$	Inverter input power values that declare the linear segments in kW.
$y_p(k)$	Inverter output power values at the ends of the linear segments in kW.
s_c	Charging coefficient factor in %.
s_d	Discharging coefficient factor in %.
P_S^{Dmax}	Storage maximum discharging power in kW.
P_S^{Cmax}	Storage maximum charging power in kW.
SOC_{min}	Minimum state of charge of the storage in kWh.
SOC_{max}	Maximum state of charge of the storage in kWh.
IC	Initial capacity of the storage in kWh.

Variables

$P_{buy}(t)$	Power absorbed from the grid in kW.
$P_{sell}(t)$	Power injected to the grid in kW.
Z	Maximum value of the variables $P_{buy}(t)$.
Y	Maximum value of the variables $P_{sell}(t)$.
$P_{Dis}(t)$	Discharging power of the storage in kW.
$P_{Ch}(t)$	Charging power of the storage in kW.
$X_{DC}(t)$	Inverter input power at the DC side in kW.
$Y_{DC}(t)$	Inverter output power at the DC side in kW.
$X_{AC}(t)$	Inverter input power at the AC side in kW.
$Y_{AC}(t)$	Inverter output power at the AC side in kW.
$SOC(t)$	State of charge of the storage in kWh.
$W(k,t)$	Auxiliary continuous variables for the piecewise linearization of the DC to AC power conversion.
$Q(k,t)$	Auxiliary continuous variables for the piecewise linearization of the AC to DC power conversion.

I. INTRODUCTION

A. Motivation and Background

The share of renewable energy sources (RES) is estimated to reach 32% by 2030 according to the European targets for climate and energy [1]. As a result, the penetration of RES into the power system is expected to continue this upward trend for the next decades. A significant share of renewables is produced by photovoltaic (PV) panels, which can be installed as small scale systems in residential or non-residential buildings or as large scale system in solar power parks. Especially for countries with abundant sunshine, PV technology will play a vital role in meeting European Union energy targets.

This work is partially supported by the European Union's Horizon 2020 research and innovation programme under grant agreement No 739551 (KIOS CoE) and the Research Promotion Foundation (RPF, Cyprus, Project KOINA/SOLAR-ERA.NET/1215/06) through the SOLAR-ERA.NET (European Union's Seventh Framework Programme).

978-1-7281-1156-8/19/$31.00 ©2019 IEEE

PV energy systems are integrated into the grid through a grid-tied inverter based on power electronics technology. However, the short lifetime of inverters is a significant drawback of PV investments. Thus, one of the main objectives set within the implementation plan of the Solar Europe Industry Initiate (SEII) [2] is to extend the lifetime of PV inverters in order to improve the competitiveness of solar energy. Another main drawback of the PV systems is related with stability, congestion, and power quality problems that can be caused in the case of massive integration of PVs into the power system. One example is the overvoltage conditions in segments and feeders of an LV distribution network due to the reverse and variable power flow imposed by the installed PVs. However, the aforementioned drawbacks of the PV systems can be addressed by the integration of Energy Storage System (ESS). ESSs are an emerging technology that can create the potentials for an optimal management of the energy produced by RES. As a result, the ESS can be used to compensate the intermittent and uncontrollable character of RES, and to control the power flow through the inverter in order to extend its lifetime. Also, ESSs create new energy market opportunities by the flexible management of electricity that allow the profit maximization.

B. *Relevant Literature*

Recent studies indicate that the expected lifetime of PV inverters is strongly related with their thermal-power loading during their operation. In [3], the expected inverter lifetime is investigated for two different mission profiles according to field measurements obtained from two different regions: USA-Arizona and Denmark-Aalborg. As an outcome of this investigation, the inverter lifetime is shown to decrease by up to 70% when the inverter is operating with unfavorable thermal-power loading. Investigation studies in [4] and [5] show that by using a constant power mode or limiting the maximum output power of the inverter to a lower value (i.e., at 80% of the rated power) can reduce the thermal loading of the inverter and double or even triple its lifetime. However, such a power limitation reduces the generated energy from PVs (significant losses due to energy shedding at the peak power) and as a result the profit from selling the energy to the grid is reduced. Now, in case where there is an available ESS at the DC link of a PV system, the excess power from the PV during peak production periods can be shifted to non-peak periods. As a result, the reduction of the PV energy production can be avoided and the profit can be increased in case of hybrid (PV-storage) systems in DC coupling configuration.

There are several examples where optimization techniques have been designed for various configurations of ESS in order to maximize the profit. A linear programming model and a mixed-integer linear programming (MILP) model are presented in [6] and [7], in order to schedule the energy of the micro-grid batteries for the next day using forecasted input data. In [8], an optimization model for the operation of smart buildings in a microgrid is proposed, and aims to minimize the total electricity cost of the microgrid. In our recent work [9], a MILP model is presented to minimize the cost of the electricity bill in a non-residential building equipped with a PV-Storage system.

Flexible functionalities of ESS can be used to compensate the problems caused by high penetration of unpredictable RES and provide support to the power system, such as peak shaving, load leveling, voltage regulation, and smoothing the output power of renewable generation [10]. The smoothing of power fluctuations and peak shaving is vital in grids with massive integration of PVs and ESSs in order to maintain the integrity and stability of the system; these issues are studied in [11] and [12]. A model predictive control (MPC) is presented in [11] for power smoothing of PV production. Also, in [12] the power fluctuations of a wind/PV/ESS are smoothed and a peak shaving is applied by absorbing energy during periods of low demand and injecting power during the peak demand.

C. *Contributions and Organization*

This paper investigates the case of a hybrid system for non-residential buildings, where a kinetic storage system (KSS) based on flywheel technology is connected at the DC link of a PV system. This work aims at developing a MILP based optimization method for scheduling the utilization of the KSS in order to extend the lifetime of the inverter, minimize the cost of the electricity bill in a non-residential building and ensure the smooth grid-interaction of the building. The flywheel storage is selected for this investigation due to the large number of charging and discharging cycles (increased lifetime) compared to chemical batteries. Therefore, extending the lifetime of the grid tied inverter is essential to enhance the reliability of the entire hybrid DC coupled system and minimize the levelized cost of electricity in such a novel configuration. To extend the inverter's lifetime, the optimization method considers a limit for the maximum power output of the inverter to 80% of its rated power (thus, the inverter lifetime can be extended by 200-300% according to [4] and [5]). Therefore, the proposed method can close the gap between the expected lifetime of existing inverters and the lifetime of the KSS reducing the maintenance cost of such configuration. The day-ahead electricity pricing, forecasted load and PV generation profiles are taken into account, and the algorithm decides when to buy or sell energy and when to charge or discharge the kinetic batteries for each 15-minute intervals of the next day. Also, the exponential efficiency curve of the inverter is included in the model and is approximated by a piecewise linear function.

The proposed optimization method supports the grid through a multi-objective function, which minimizes the electricity cost while also minimizing the peak power exchange with the grid, for a smooth power interaction with the grid. Further, a peak shaving is applied through the proposed optimization method since power is absorbed during periods of low electricity cost - low demand and power is injected to the grid during periods of high electricity cost - peak demand. The main contributions of this work are the following:

a) A multi-objective MILP model which maximizes the profit out of such a hybrid system, minimizes the peak power exchange with the grid and at the same time ensures an extended inverter lifetime. It also avoids any energy-profit losses due to the imposed maximum power limits.
b) A MILP model that treats the inverter operation constraint using the variables of the piecewise approximation which form a Special Ordered Set of type 2 (SOS2). As a result, any integer decision variables are avoided and therefore a great computational advantage is gained.

The rest of this paper is organized as follows. In Section II, the system description is given, followed by the problem formulation in Section III. Simulation results are presented in Section IV and the conclusions are given in Section V.

II. SYSTEM DESCRIPTION

The system under study is essentially a non-residential building that is interconnected with the power grid and is presented in Fig. 1. The non-residential building comprises of three photovoltaic-storage-inverter sub systems connected in parallel, and the building loads. Each sub system consists of 20 PV panels connected in series with a maximum power of 5 kW, a flywheel storage with 6 kWh usable capacity range and 3 kW maximum charging-discharging power [13]. Further, the 5 kVA hybrid inverter which is included in the sub system is assumed to deliver only active power during its operation [14]. The total aggregated PV capacity of the system is 15 kW, the total usable capacity of the flywheels storage is 18 kWh with 9 kW maximum charging-discharging rate, and the total maximum power of the inverters is 15 kW. The total maximum power from the PV and the flywheel storage can reach 24 kW which is higher than the maximum power of the inverters. As a result, the inverters limit the total power from the PV and the flywheel storage under the 15 kW limit. It can be noted that the maximum power of the inverters is selected to be the same with the maximum PV generation in order to reduce the capital investment of the system.

The bi-directional power flow between the AC and DC side is allowed through the hybrid inverter. Power from the grid can be absorbed to feed the load or even to charge the flywheel storage on the DC side. The flywheel storage can also be charged directly from the power generated by the PVs through the DC-link. The PV output power and the discharging power of the storage is consumed by the load and the extra power is injected into the power grid. However, the hybrid inverters are not ideal but present losses according to the inverter efficiency curve of Fig. 2(a). The efficiency curve determines how much of the DC power is converter to AC power and vice versa. Further, losses are presented in the flywheel storage according to their 92% round-trip efficiency. As a result, their charging and discharging coefficients are set to 96% in the simulations.

A PV curve for a sunny day is illustrated in Fig. 2(b), according to real measurements from a PV plant. Fig. 2(c)

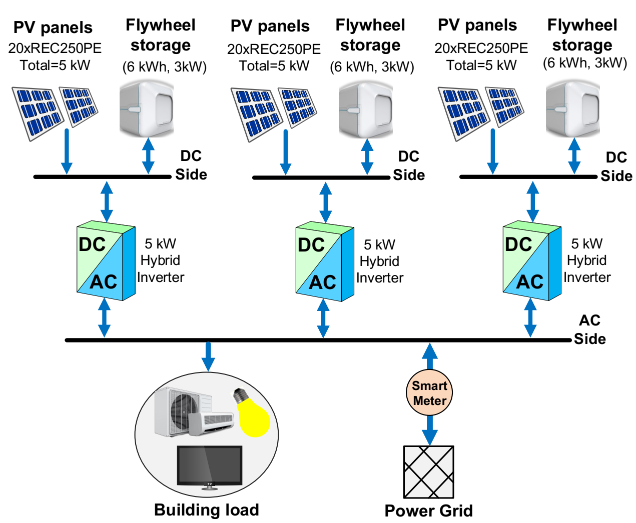

Figure 1. System description.

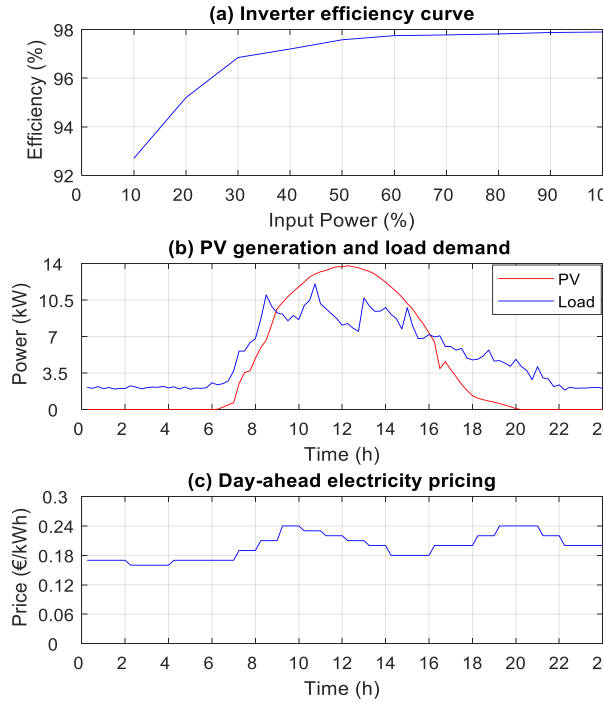

Figure 2. Input data

shows the day-ahead electricity pricing and is assumed to be the same for both electricity purchase and selling. Finally, the daily load of an office building is shown in Fig. 2(b), according to a measurement campaign performed by the authors. As can be seen in Fig. 2(b), the load is high only during working hours because of the heating or cooling load of the building and the consumption of office equipment. Note that the daily load of a non-residential building is quite predictable and follows a certain pattern.

III. PROBLEM FORMULATION

The equivalent model for formulating the optimization problem is shown in Fig. 3. In this model, single components are used to represent the system components of each category by using their aggregated values. The inverter divides the system in two areas: the AC side and the DC side. On the AC side, the power grid and the load are connected on the AC bus. Similarly, the PV and the flywheel storage are connected on the DC bus of the DC side. The arrows indicate the possible power flows in the system. Finally, the imported power in the inverter in both sides X_{DC} and X_{AC} is multiplied by the inverter efficiency curve of Fig. 2(a). Note that the exponential efficiency curve of the inverter introduces nonlinearities that make computations hard to tackle. In order to simplify the problem, the exponential efficiency curve is approximated by a piecewise linear function, and the approximation accuracy is adjusted by the number of the linear segments.

Taking into account the aforementioned approximation, the optimization problem is formulated as a mixed-integer linear programming (MILP) along an arbitrary time horizon T. The time horizon is set to one day, with 15- minute time slots. The MILP problem is solved to optimality and computes the power flow in the system that minimizes the electricity bill of the

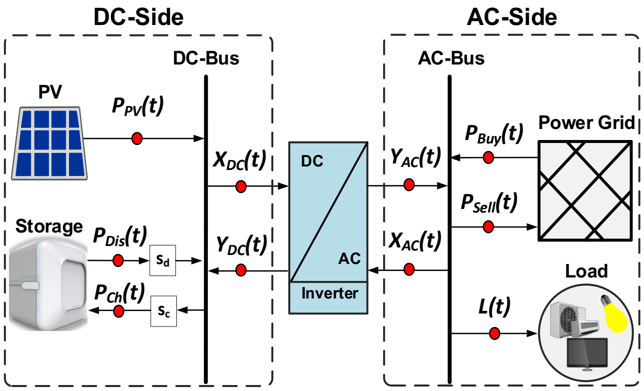

Figure 3. Equivalent model of the system.

building and the maximum power exchange with the grid, while satisfying the power balance of the system and the maximum operational limit of the inverter. It must be noted that deterministic forecasted data values for load, day ahead electricity pricing, and the PV generation are used in this paper.

A. Objective Function

The multi-objective function of the resulting optimization problem is presented in (1) and the objective is to minimize the cost of electricity bill in the building according to (2) and to minimize the maximum absorbed and injected power to the grid according to (3) for the whole period of study. In (2), the profit from selling power to the grid should be maximized and the cost of buying power from the grid should be minimized.

$$\min f = w_1 f_1 + w_2 f_2 + w_3 f_3 \tag{1}$$

$$f_1 = \sum_{t=1}^{T} \left(\frac{c_{buy}(t)}{4} P_{buy}(t) - \frac{c_{sell}(t)}{4} P_{sell}(t) \right) \tag{2}$$

$$f_2 = \max_t P_{buy}(t)\,, \quad f_3 = \max_t P_{sell}(t) \tag{3}$$

where w_1, w_2, and w_3 are weight coefficients. Note that the cost parameters are divided by 4 due to the 15-minute time slots in order to be associated for each fraction of time. Furthermore, in the case where the cost of buying and selling electricity is the same, then an infinitesimally small constant can be added in one of the two cost parameters in order to avoid the simultaneous power injection and absorption with the power grid. Note that by adjusting the weight coefficients, the solution of this optimization problem can be beneficial only for the prosumer ($w_1 \neq 0,\ w_2 = 0$ and $w_3 = 0$), only for the grid ($w_1 = 0,\ w_2 \neq 0$ and $w_3 \neq 0$) or for both parties ($w_1 \neq 0,\ w_2 \neq 0$ and $w_3 \neq 0$).

The objective function in (1) with the minimax functions is reformulated in (4), and subjected to several operational constraints and limitations.

$$\min\ f = w_1 \sum_{t=1}^{T} \left(\frac{c_{buy}(t)}{4} P_{buy}(t) - \frac{c_{sell}(t)}{4} P_{sell}(t) \right) + w_2 Z + w_3 Y \tag{4}$$

B. Constraints

1) Minimax objectives: The following constraint guarantees that by minimizing variables Z and Y, then these variables will be assigned the maximum value of these expressions.

$$P_{buy}(t) \leq Z, \quad P_{sell}(t) \leq Y \qquad \forall t \in T \tag{5}$$

2) Power balance: In (6), the input power in the DC-Bus must be equal to the output power of the DC-Bus. Similarly, the input power in the AC-Bus must be equal to the output power of the AC-Bus according to (7).

$$\begin{aligned} &P_{PV}(t) + P_{Dis}(t) + Y_{DC}(t) = P_{Ch}(t) + X_{DC}(t) \quad \forall t \in T \\ &0 \leq P_{Dis}(t) \leq P_S^{Dmax}, \ \ 0 \leq P_{Ch}(t) \leq P_S^{Cmax} \quad \forall t \in T \end{aligned} \tag{6}$$

$$P_{buy}(t) + Y_{AC}(t) = L(t) + P_{sell}(t) + X_{AC}(t) \quad \forall t \in T \tag{7}$$

3) State of charge of the storage: The state of charge of the storage in time is measured in kWh and is expressed as the initial capacity of the storage minus the summation of the discharging power plus the summation of the charging power for all the past and the present time intervals. The charging and discharging power is divided by 4 due to the 15 min time slots, in order to be associated for each fraction of time. Note that the charging and discharging of the storage cannot occur at the same time interval due to the charging and discharging losses.

$$\begin{aligned} &SOC(t) = IC + \frac{1}{4} \sum_{j=1}^{t} \left(s_c \times P_{Ch}(j) - \frac{P_{Dis}(j)}{s_d} \right) \ \forall t \in T \\ &SOC_{min} \leq SOC(t) \leq SOC_{max} \quad \forall t \in T \end{aligned} \tag{8}$$

4) Inverter output power: The output power of the inverter is the product of the inverter input power and the efficiency curve of Fig. 2(a). In this work, five linear segments (N=5) are used for the piecewise approximation of the efficiency curve.

$$\begin{aligned} X_{DC}(t) &= \sum_{k=1}^{N} W(k,t) \times x_p(k) \quad \forall t \in T \\ Y_{AC}(t) &= \sum_{k=1}^{N} W(k,t) \times y_p(k) \quad \forall t \in T \end{aligned} \tag{9}$$

$$\begin{aligned} X_{AC}(t) &= \sum_{k=1}^{N} Q(k,t) \times x_p(k) \quad \forall t \in T \\ Y_{DC}(t) &= \sum_{k=1}^{N} Q(k,t) \times y_p(k) \quad \forall t \in T \end{aligned} \tag{10}$$

$$\sum_{k=1}^{N} W(k,t) = 1\,, \sum_{k=1}^{N} Q(k,t) = 1 \quad \forall t \in T \tag{11}$$

where x_p are set to 0%, 0.1%, 10%, 30%, 50% and 100% and are multiplied by the maximum input power of the inverter; y_{points} are set to 0%, 0%, 92.7%, 96.8%, 97.5% and 97.9% and are multiplied by the maximum input power of the inverter; $W(k,t)$ and $Q(k,t)$ range between 0 and 1 and form an SOS2, which means that at most two variables can be non-zero, and these two variables must be adjacent in ordering given to the set, thus defining one of the line segments. It is assumed that the efficiency of the inverter is increased linearly from 0% to

92.7% when the inverter operates from 0% to 10% of its nominal power. Note that the linear segment between 0% and 0.1% of the inverter input power is unnecessary for the piecewise approximation, however it is introduced for the restriction of the inverter operation in the next constraint.

5) Inverter operation restriction: The power flow through the inverter must be in one direction at each time interval and can be achieved through the piecewise approximation where we force the inverter to work at first segment (zero output power) for at least of one of its two modes (AC to DC and DC to AC power conversion). Note that the inverter operation restriction can also be satisfied using integer variables. However, using the proposed formulation we treat these restrictions as an SOS2 set, which is treated algorithmically by the solver, thus greatly improving the computational time [15].

$$W(k=1,t) + Q(k=1,t) \geq 1 \quad \forall t \in T \tag{12}$$

IV. SIMULATION RESULTS

In this section, the proposed mathematical formulation is coded in MATLAB and a commercial solver solves the MILP problem. Several case scenarios are examined to illustrate the optimized energy scheduling of the building and to compare the electricity cost and the maximum power exchange with the grid for three different objectives which are the profit maximization, the grid support, and the lifetime extension. The combinations of these objectives are also examined. The day-ahead electricity pricing, load and the PV curve are used as input data.

The optimized energy scheduling of the building where the inverter maximum power is set at 80% of its rated power in order to reduce the thermal loading of the inverter for enhancing its lifetime is presented in Figs 4, 5 and 6. Fig. 4 indicates the case where the objective is only to minimize the electricity cost of the building, Fig. 5 presents the case where the objective is only to minimize the power exchange with the grid. The multi-objective case of minimizing the electricity cost and the power

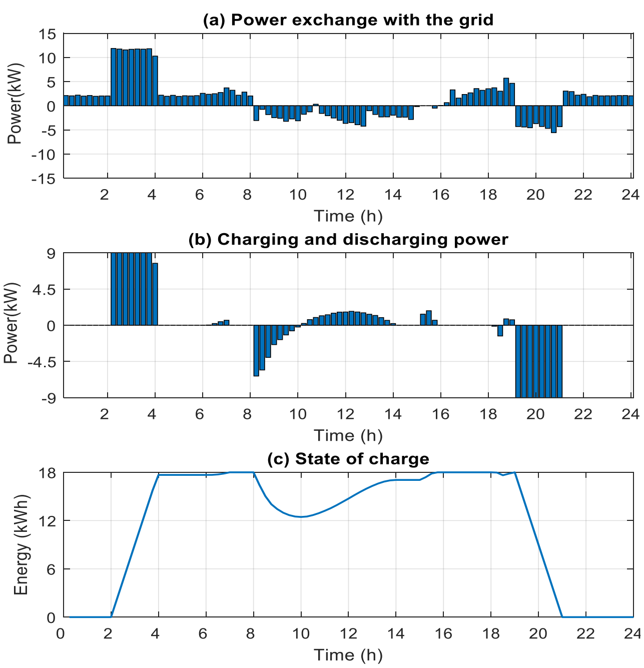

Figure 4. Profit maximization.

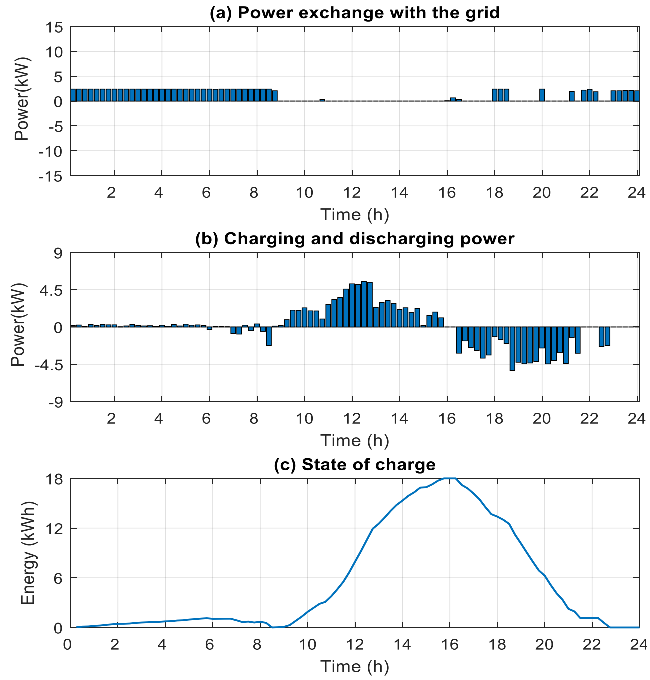

Figure 5. Grid power exchange minimization.

exchange with the grid is shown in Fig. 6. Also, Figs 4(a), 5(a) and 6(a) illustrate the power absorption (positive values) from the grid and the power injection (negative values) into the grid. Similarly, Figs 4(b), 5(b) and 6(b) show the charging (positive values) and discharging power (negative values) of the storage. Further, Figs 4(c), 5(c) and 6(c) indicate the state of charge of the storage. Initially, the storage capacity is zero. As it is expected in the cases of the profit maximization, power is absorbed from the grid and the storage is charged during periods of low electricity cost. Conversely, the storage is discharged and power is injected into the grid during periods of high electricity cost. However, in these cases the PV production exceeds the maximum power limitation of the inverter between 10 am to 2 pm (12 kW; 80%). As a result, the storage is charged from the PV excess power as can be seen in Figs 4(b) and 6(b).

The results of the simulations are summarized in Table I. The first two results refer to the cases without storage and the proposed optimization algorithm. Then, the produced power from the PVs is consumed at the load and the surplus power is injected to the grid immediately. In these cases, the daily electricity cost increases by 17% (4.83 to 5.82 €) in the case where the lifetime extension of the inverter is considered, and

TABLE I. SIMULATION RESULTS

Profit maximization	Grid support	Lifetime extension	Daily electricity cost (€)	Max. absorbed power (kW)	Max. injected power (kW)
×	×	×	4.83	4.91	5.82
×	×	✓	5.82	4.91	4.25
×	✓	×	5.25	2.43	0
×	✓	✓	5.19	2.41	0
✓	×	×	3.45	11.88	7.17
✓	×	✓	3.87	11.86	5.57
✓	✓	×	3.71	5.32	5.65
✓	✓	✓	4.13	3.72	4.24

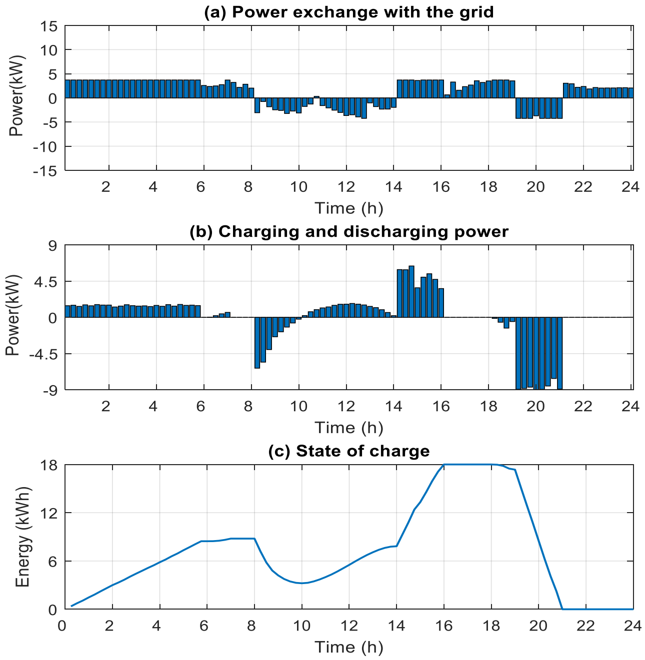

Figure 6. Profit maximization and grid power exchange minimization.

this due to the 4.79 kWh PV energy losses during the saturation period of the inverter. The next two results consider the cases of the grid support due to the minimization of the maximum power exchange with the grid. As a result, the smoothing of the power interaction with the grid and the maximum absorbed power of 2.4 kW are presented in Fig. 5(a). However, the daily electricity cost is very high in these situations (approximately 5.2 €). Note that the consideration of the inverter lifetime extension does not affect the results of the grid support because the inverter operates at lower operating levels. Further, the consideration of the profit maximization leads to the lowest daily electricity cost of 3.45 € and 3.87 € without and with the inverter lifetime extension respectively. However, in order to minimize the electricity cost, the power exchange with the grid is extremely high and reaches 11.8 kW.

The multi-objective solution of the proposed optimization problem is suggested. This considers the profit maximization and the grid support and manages to reduce significantly the daily electricity cost to 3.71 and 4.13 € (1.12 and 1.69 € less than the non-optimized case). Also, the maximum absorbed power is maintained at 5.32 and 3.72 kW without and with the inverter lifetime extension respectively. Further, these results are 7% and 6% (0.26 and 0.26 €) higher in terms of the electricity cost and 55.2% and 68.7% (6.56 and 8.16 kW) less in terms of the maximum power exchange with the grid, compared to the case where the profit maximization is only considered. Moreover, these results are 29.3% and 20.4% (1.54 and 1.06 €) less in terms of the electricity cost and 54.3% and 35.2% (2.89 and 1.31 kW) higher in terms of the maximum power absorbed, compared to the case where the grid support is only considered. As a result, with a small increment at the daily electricity cost we manage to reduce significantly the maximum power exchange with the grid and therefore to smooth the power interaction with the grid for benefiting both the prosumer and the power grid. Also, using the multi-objective solution, a peak shaving is applied. Note that by adjusting the weights ($w_1 = 1, w_2 = 8$ and $w_3 = 3$ in this simulation) in (1), the solution can be more beneficial for the prosumer, the grid or it can be equally beneficial for both.

The multi-objective solution of the proposed optimization problem considers the inverter lifetime extension (200-300%) by a small cost increment of 0.44 € (annual cost of 160.6 €). However, there is a significant gain due to the extended inverter lifetime (by avoiding 1-2 replacements of the inverters during the investment lifetime). The cost for replacing the hybrid inverter is considered to be much higher than the cost due to the maximum power reduction. Thus, the proposed techniques for the specific system configuration are very beneficial.

V. CONCLUSION

In this paper, a multi-objective optimization technique is proposed for scheduling the utilization of the KSS in order to extend the lifetime of the inverter, to minimize the cost of the electricity bill and to reduce the peak power exchange with the grid in a non-residential building equipped with a PV-Storage system. Results show that the daily electricity cost of the building and the maximum power exchange with the grid are minimized and therefore the power interaction with the grid is smoothed to benefit both the prosumer and the power grid. The extension of the proposed model to a stochastic model is part of our future work, in order to address forecasting uncertainties.

REFERENCES

[1] European Commission, "Europe 2030 climate strategies and targets,".
[2] Solar Europe Industry Initiative (SEII), "PV implementation plan 2013-2015," May 2013.
[3] N. C. Sintamarean et al., "Reliability oriented design tool for the new generation of grid connected PV-inverters," *IEEE Trans. Power Electronics*, vol. 30, no. 5, May 2015, pp. 2635-2644.
[4] Y. Yang, H. Wang, F. Blaabjerg and T. Kerekes, "A hybrid power control concept for PV inverters with reduced thermal loading," *IEEE Trans. Power Electr.*, vol. 29, no. 12, Dec. 2014, pp. 6271-6275.
[5] Y. Yang et al., "Pursuing photovoltaic cost-effectiveness: absolute active power control offers hope in single-phase PV systems," *IEEE Industry Applications Magazine*, vol. 23, no. 5, Sep.-Oct. 2017, pp. 40-49.
[6] P. Mahat, "A micro-grid battery storage management," in *Proc. IEEE PES General Meeting*, Vancouver, Canada, 2013, pp. 1-5.
[7] A.C. Luna et al., "Mixed-integer-linear-programming-based energy management system for hybrid PV-wind-battery microgrids: modeling, design, and experimental verification," *IEEE Trans. Power Electronics*, vol. 32, no. 4, Apr. 2017, pp. 2769-2783.
[8] J. A. Pinzon et al., "Optimal management of energy consumption and comfort for smart buildings operating in a microgrid," *IEEE Trans. Smart Grid*, vol. 10, no. 3, May 2019, pp. 3236-3247.
[9] L. Tziovani et al., "Energy scheduling in non-residential buildings integrating battery storage and renewable solutions," in *Proc. IEEE ENERGYCON*, Limassol, Cyprus, 2018, pp. 1-6.
[10] W. Choi et al., "Reviews on grid-connected inverter, utility-scaled battery energy storage system, and vehicle-to-grid application - challenges and opportunities," in *Proc. IEEE ITEC*, Chicago, IL, USA, 2017, pp. 203-210.
[11] M. Lei et al., "An MPC-based ESS control method for PV power smoothing applications," in *IEEE Trans. Power Electronics*, vol. 33, no. 3, Mar. 2018, pp. 2136-2144.
[12] L. Pan, J. Gu, J. Zhu and T. Qiu, "Integrated control of smoothing power fluctuations and peak shaving in Wind/PV/Energy Storage System," in *Proc. IHMSC*, Hangzhou, 2016, pp. 586-591.
[13] Technical specification of Kinetic Battery – EQ 3000, [Online]. Available: www.chakratec.com
[14] Fronius Symo Hybrid 5.0-3-S, [Online]. Available: http://www.fronius.com/en/photovoltaics/products/home/inverters/fronius-symo-hybrid
[15] H. Paul Williams, *Model Building in Mathematical Programming*, 5th ed. John Wiley & Sons, 2013, p. 178.